Geophysical Journal International

Geophys. J. Int. (2012) **190,** 59–74 doi: 10.1111/j.1365-246X.2012.05493.x

Seismic hazard along the southern boundary of the Gônave microplate: block modelling of GPS velocities from Jamaica and nearby islands, northern Caribbean

B. Benford,[1] C. DeMets,[1] B. Tikoff,[1] P. Williams,[2] L. Brown[2] and M. Wiggins-Grandison[3]

[1] *Department of Geoscience, University of Wisconsin—Madison,* 1215 *W. Dayton St., Madison, WI* 53706, *USA. E-mail: bryn@geology.wisc.edu*
[2] *Earthquake Unit, University of the West Indies, Mona Campus, Kingston* 7, *Jamaica*
[3] *Preparatory Commission for the Comprehensive Nuclear-Test Ban Treaty Organization, Vienna International Centre, P.O. Box* 1250, 1400 *Vienna, Austria*

Accepted 2012 April 3. Received 2012 April 1; in original form 2012 January 4

SUMMARY

We use block modelling of GPS site velocities from Jamaica and nearby islands, including Hispaniola, to test alternative plate boundary geometries for deformation in Jamaica and estimate slip rates along the island's major fault zones. Relative to the Caribbean Plate, GPS sites in northern Jamaica move 6.0 ± 0.5 mm yr^{-1} to the WSW, constituting a lower bound on the motion of the Gônave microplate across its southern boundary in Jamaica. Obliquely convergent motion of all 30 GPS sites on and near Jamaica relative to the island's ∼E–W-trending strike-slip faults may be partitioned into 2.6 ± 0.6 mm yr^{-1} of ∼N–S shortening across submarine faults south of Jamaica and 5–6 mm yr^{-1} of E–W motion. Guided by geological and seismic information about the strikes and locations of faults in Jamaica, inverse block modelling of the regional GPS velocities rejects plate boundary configurations that presume either a narrow plate boundary in Jamaica or deformation concentrated across a restraining bend defined by the topographically high Blue Mountains of eastern Jamaica. The best-fitting models instead place most deformation on faults in central Jamaica. The 4–5 mm yr^{-1} slip rate we estimate for the Plantain Garden fault and Blue Mountain restraining bend of southeastern Jamaica implies significant seismic hazard for the nearby capital of Kingston.

Key words: Plate motions; Dynamics and mechanics of faulting; Neotectonics; Fractures and faults.

1 INTRODUCTION

The 2010 January 12, $M = 7$ Haiti earthquake (Calais *et al.* 2010; Hayes *et al.* 2010), which ruptured an on-land segment of the southern boundary of the Gônave microplate (Fig. 1), was a tragic reminder that the strike-slip faults that define much of the northern boundary of the Caribbean Plate constitute major seismic hazards where those faults come on land (Prentice *et al.* 2010). The island of Jamaica (Fig. 1), which lies along the same seismically active plate boundary, has had 12 earthquakes with Modified Mercalli intensities (MMI) of VII to X since 1667, including the MMI X earthquake in 1692 that destroyed much of the city of Port Royal (near the present capital of Kingston) and the $M = 6$–6.5 earthquake in 1907 that damaged or destroyed 85 per cent of the buildings in Kingston (Taber 1920; Versey *et al.* 1958; Pereira 1977; Tomblin & Robson 1977; Clark 1995; Wiggins-Grandison 1996; Natural Disaster Research 1999; Wiggins-Grandison 2001). Despite Jamaica's long history of damaging earthquakes, remarkably little is known about which faults were responsible for previous large earthquakes and which faults presently constitute the most significant seismic hazards, including the locations of the 1692 and 1907 ruptures.

In an effort to better understand seismic hazard and deformation rates in Jamaica, GPS measurements began on the island in 1998. DeMets & Wiggins-Grandison (2007) (hereafter abbreviated DWG07) report the initial results from these measurements along with focal mechanisms determined from teleseismic and local seismograms. DWG07 demonstrate that GPS sites move dominantly to the WSW relative to a stationary Caribbean Plate at rates that increase from 3 mm yr^{-1} in southern Jamaica to 7–8 mm yr^{-1} in northern Jamaica and further demonstrate that the mean *P*- and *T*-axes for earthquakes on and near the island have nearly horizontal plunges and trend 45° from the island's E–W-oriented strike-slip faults (Fig. 2c). From these observations, they conclude that deformation in Jamaica is dominated by a combination of left-lateral shear along E–W striking strike-slip faults and convergence across the island's NNW-striking mountain ranges, both consistent with a general model of the island as a major restraining bend in the left-slipping Gônave–Caribbean Plate boundary (Mann *et al.* 1985).

Herein, we build on the DWG07 study by modelling GPS velocities estimated from 13 yr of continuous and campaign GPS measurements at 30 Jamaican sites and 96 sites in Hispaniola (Manaker *et al.* 2008; Calais *et al.* 2010) and other islands that

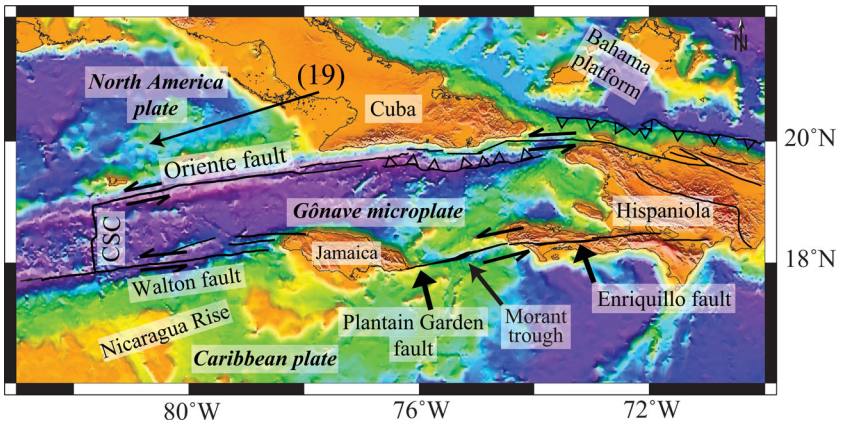

Figure 1. Tectonic setting of Jamaica and vicinity. Jamaica is located in a restraining bend on the left-lateral strike-slip boundary between the Caribbean Plate and the Gônave microplate. Arrow shows MORVEL estimate of North America Plate motion in mm yr^{-1} relative to the Caribbean Plate (DeMets *et al.* 2010). CSC, Cayman spreading centre. 2 min seafloor bathymetry and land topography are from Sandwell & Smith (1997).

span the Caribbean–Gônave–North America Plate boundary. Using the locations of major faults and earthquakes in Jamaica and the northern Caribbean as a guide, we test a series of progressively more complex models for the geometry of the Gônave–Caribbean Plate boundary in Jamaica, ranging from simple discrete/narrow boundaries to boundaries with an independently moving block in Jamaica. Based on our preferred plate boundary geometries, we estimate present-day fault slip rates and the locus of present deformation in Jamaica. Modelling of the GPS velocity field is accomplished using the Blocks software of Meade & Loveless (2009), which treats the crust as an elastic homogeneous half-space consisting of rotating blocks bound by frictionally locked plate-boundary faults.

2 TECTONIC SETTING

2.1 Gônave microplate

Jamaica straddles the boundary between the Gônave microplate and Caribbean Plate (Fig. 1) and is located at the northern, emergent end of the Nicaragua Rise (Fig. 1), where the rise collides obliquely with the southern edge of the Gônave microplate. Westward motion of 8–13 mm yr^{-1} of the Gônave microplate relative to the Caribbean Plate (DWG07), likely driven by the oblique collision of the Bahama platform with Hispaniola (Mann *et al.* 1995, 2002), gives rise to left-lateral slip on the Enriquillo, Plantain Garden and Walton faults along the southern edge of the Gônave microplate (Fig. 1).

The Gônave microplate boundaries consist of the Cayman spreading centre in the west, the Oriente transform fault in the north, multiple faults in the south including the Enriquillo fault of Hispaniola, the Plantain Garden fault, faults in Jamaica and the Walton fault west of Jamaica (Fig. 1; Rosencrantz & Mann 1991; Tyburski 1992). The eastern boundary of the microplate may lie west of Hispaniola, within central Hispaniola or may be diffuse (Manaker *et al.* 2008; Calais *et al.* 2010; Benford *et al.* 2012a).

2.2 Faults in Jamaica

The ∼50 km right step between the Plantain Garden fault (PG) of eastern Jamaica and Walton fault (WF) west of Jamaica define the Jamaica restraining bend (Fig. 2a). The right-stepping Jamaica restraining bend has given rise to widespread faulting and reactivation of faults in and near Jamaica consisting of east–west striking, left-lateral strike-slip faults and NNW-striking faults dominated by reverse dip-slip motion (Figs 1 and 2a; Horsfield 1974; Wadge & Dixon 1984; Mann *et al.* 1985; Leroy *et al.* 1996). The latter faults are typically steeply east-dipping, in many cases are blind, and are Palaeogene extensional structures reactivated in contraction (Horsfield 1974; Draper 2008).

Previous studies (Horsfield 1974; Wadge & Dixon 1984; Mann *et al.* 1985; Leroy *et al.* 1996; DeMets & Wiggins-Grandison 2007) of the structures and topography of Jamaica define four major, east–west striking, left-lateral strike-slip fault systems on the island (Fig. 2a), the Duanvale fault (DF) of northern Jamaica, the South Coast fault zone (SCFZ) of southern Jamaica, the Plantain Garden and Aeolus Valley (AV) faults of southeastern Jamaica and the central Jamaica fault system, consisting of the Cavaliers fault (CF), Rio Minho-Crawle River fault (RMCR) and Siloah fault system (SFS). None of these east–west faults have the typical geomorphic expression of a large-offset, strike-slip fault (e.g. fault scarps, sag ponds) and none can be traced continuously across the island. However, they show up as prominent lineaments in aerial photographs and in the 90-m Shuttle Radar Topography Mission (SRTM) elevations (Fig. 2b). Below, we describe each briefly.

The Plantain Garden fault extends ∼150 km from the Morant Trough (Fig. 1), an active pull-apart basin east of Jamaica (Mann *et al.* 1990) that defines the western termination of the Enriquillo fault of Hispaniola, to the Wagwater deformed belt (WW in Fig. 2b) at the western edge of the Blue Mountains (Mann *et al.* 1985). Estimates of the fault offset east of the island range from 30 to 45 km based on the offset of the eastern Jamaica shelf to ∼60 km based on the width of the Morant Trough. These are consistent with 3–7 mm yr^{-1} of slip on the Plantain Garden fault assuming the offset has occurred since ∼9 Ma (Natural Disaster Research 1999). Farther west, where the Plantain Garden fault of eastern Jamaica separates the Blue Mountains to the north from topographically lower and younger rocks to the south, rocks of similar ages and lithologies flanking the fault are offset by only 10–12 km (Mann *et al.* 1985).

The difference in the offsets estimated for the eastern and western halves of the Plantain Garden fault may be because of partitioning of slip between the western segment of the Plantain Garden fault and a

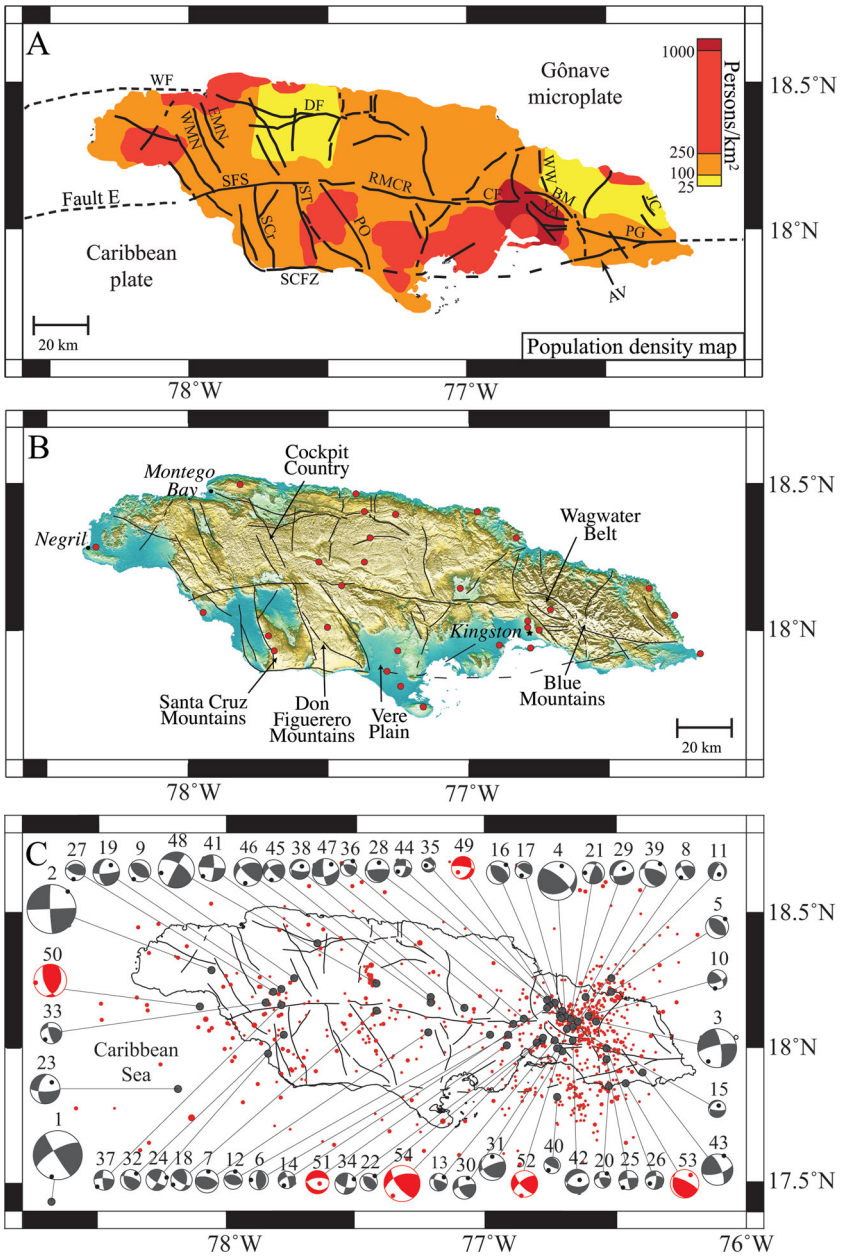

Figure 2. (a) Major faults of Jamaica modified from Wiggins-Grandison & Atakan (2005) and Benford *et al.* (In preparation, 2012b). Long-dashed line shows assumed offshore continuation of the Aeolus Valley fault. NNW-striking faults are BM, Blue Mountain fault; JC, John Crow fault; PO, Porus fault; ST, Spur Tree fault; SCr, Santa Cruz fault; WMN and EMN, Western and Eastern Montpelier-Newmarket faults, respectively and WW, Wagwater Belt. Strike-slip faults are: AV, Aeolus Valley fault; CF, Cavaliers fault; DF, Duanvale fault; PG, Plantain Garden fault; RMCR, Rio Minho-Crawle River fault; SCFZ, South Coast fault zone; SFS, Siloah fault system; WF, Walton fault; YA, Yallahs fault and approximate location of Fault E of the Walton fault (Tyburksi 1992). The CF, RMCR and SFS constitute the central Jamaica fault system. Faults are overlain on a population density map as of 2007. Faults are also shown in panels (b) and (c). (b) Locations of major cities, including the capital city of Kingston, and major geographic features. GPS station locations (red circles) on 90-m Space Shuttle Topographic Radar Mission topography illuminated from the southwest. (c) Earthquakes from the International Seismological Centre for the period 2000–2010 (June); magnitudes range from 2.0 to 5.9. Earthquake focal mechanisms #1–2 are from Van Dusen & Doser (2000), #3–4 from Wiggins-Grandison (2001), #5–48 from DeMets & Wiggins-Grandison (2007) and #49–54 (shown in red) from the ISC for the period 2005–2008. Focal mechanism parameters for events #49–54 are given in Table 1. Focal mechanisms are scaled to magnitude. Black or red dots in the focal mechanisms indicate pressure axes.

previously undescribed, unnamed WSW-striking fault that is visible in both aerial photographs and 90-m SRTM elevations (Figs 2a and b; AV). Hereafter, we refer to this fault as the Aeolus Valley fault for the valley in eastern Jamaica where the fault is located (Figs 2a and b). The fault, which is mapped but not named on the 1992 Jamaica Mining and Commerce structure maps, intersects the eastern Plantain Garden fault and may carry motion offshore to the South Coast fault zone (Fig. 2a; SCFZ).

In northern Jamaica, the Duanvale fault (DF) has a locally prominent topographic signature, where it is lower than the surrounding areas and creates a lineament at the macroscale (Wadge & Dixon 1984). The small offset estimated across the Duanvale fault, less

Table 1. Earthquake source parameters.

Code[a]	Date (year.month.day)	Hypocentre			M_d	Focal mechanism		
		Latitude (°N)	Longitude (°E)	Depth (km)		Strike	Dip	Rake
49	2005.09.24	18.12	−76.70	12	3.2	278	77	−59
50	2006.02.13	18.15	−78.13	24	3.8	159	62	67
51	2007.12.15	18.00	−76.94	15	2.8	114	33	−62
52	2008.06.11	18.07	−76.66	3	3.1	234	68	20
53	2008.06.26	17.88	−76.46	17	3.4	296	76	75
54	2008.07.14	18.02	−76.78	11	3.9	249	52	27

Note: M_d are earthquake duration magnitudes. Strike is measured clockwise from north. Dip is measured in degrees clockwise about the strike. Rake is measured as degrees counter-clockwise from strike in the specified nodal plane.
[a]Focal mechanism codes are tied to Fig. 2(c).

than 10 km and as little as 3 km (Wadge & Dixon 1984), based on offset of Cretaceous units (Grippi 1978), either argues against this fault as a primary plate boundary structure or indicates that it became active too recently to accumulate significant offset. We test these possibilities below.

The left-lateral Rio Minho-Crawle River fault (RMCR) of central Jamaica offsets Cretaceous features in the Central Inlier by 8 km, is reactivated from the Cretaceous (Mitchell 2003) and is the most seismically active strike-slip fault on the island (Fig. 2; DeMets & Wiggins-Grandison 2007). Field mapping, structure maps and topographic maps define the Siloah fault system (SFS) west of the Cavaliers and Rio Minho-Crawle River faults; these three faults define a continuous central Jamaica fault system (Benford *et al.*, Fault interaction of reactivated faults within a restraining bend, southern Jamaica, In preparation, 2012b; Fig. 2). The Siloah fault system is a reactivated fault from the Eocene (Wright 1975). No reverse faults or mountain ranges are continuous across the central Jamaica fault system at the 90-m SRTM-scale or based on fieldwork.

The South Coast fault zone (SCFZ) cuts across the alluvium-covered Vere Plain of south–central Jamaica and closely parallels the southern coast of southwestern Jamaica, where it creates prominent cliffs as it crosscuts the NNW-oriented ranges that occur to the north. The cliffs associated with the South Coast fault zone extend along the western third of the island. Offset is not constrained for the South Coast fault zone.

North–northwest-striking faults are interpreted as dip-slip features (Fig. 2a; Horsfield 1974). In eastern Jamaica, the Blue Mountain and Yallahs faults accommodate some or all contraction across the Blue Mountains, which are Jamaica's highest (>2000 m) and most seismically active region (Fig. 2). Farther west, uplift of the Don Figuerero Mountains and Santa Cruz Mountains, which reach ∼800 m and ∼660 m, respectively, occurs along NNW-striking reverse faults (Fig. 2). Recent mapping by Benford *et al.* (In preparation, 2012b) shows that these NNW-striking ranges are cored by east-dipping reverse faults that terminate at and are bounded by the South Coast fault zone in the south and the central Jamaica fault system in the north.

3 GEODETIC DATA

3.1 Jamaica GPS network description

The Jamaica GPS network consists of 30 geodetic benchmarks (Table 2; Fig. 3), 28 on the main island of Jamaica and one each on Morant Cay and Pedro Cay. GPS data described and used by DWG07 include data from 20 sites spanning the period 1998–2005; the present velocity field includes 18 of the 20 sites used by DWG07 and 12 new sites, notably including two sites on limestone cays, 50 km southeast and 80 km south of the main island (MCAY and PEDR in Fig. 3a). Data for the present study span a 13-yr-long period from 1998 to 2011 August (Table 2). The velocities for GPS stations BAMB and COFE used by DWG07 are omitted from this study because of concerns about the stability of these two sites. Continuous or quasi-continuous measurements constrain the velocities at 6 of the 30 sites (Table 2); the remaining station velocities are derived from campaign measurements, typically lasting five or more days per site occupation (Table 2). All data from the Jamaica GPS sites are available through UNAVCO (University NAVSTAR Consortium) or the National Geodetic Survey CORS archive.

3.2 GPS data analysis

Except for the data for stations from Hispaniola, whose velocities are taken from Calais *et al.* (2010), all the GPS data used for this study were processed with Release 6.1 of the GIPSY software suite from the Jet Propulsion Laboratory (JPL). Non-fiducial daily GPS station coordinates were estimated using a precise point-positioning strategy (Zumberge *et al.* 1997), including constraints on *a priori* tropospheric, hydrostatic and wet delays from Vienna Mapping Function (VMF1) parameters (http://ggosatm.hg.tuwien.ac.at), elevation-dependent and azimuthally dependent GPS and satellite antenna phase centre corrections from IGS08 ANTEX files (available via ftp from sideshow.jpl.nasa.gov) and corrections for ocean tidal loading from the TPX0.7.2 ocean tide model (http://froste.oso.chalmers.se). Wide- and narrow-lane phase ambiguities were resolved for all the data using GIPSY's single-station ambiguity resolution feature.

All daily non-fiducial station location estimates were transformed to ITRF2008 (Altamimi *et al.* 2011) using daily 7-parameter Helmert transformations from JPL. The resulting station coordinate time-series have day-to-day scatter of 2.8 and 3.1 mm yr^{-1} in their latitudes and longitudes, respectively, relative to simple linear-fit models. We further estimated and removed common-mode noise for all the stations using noise common to the coordinate time-series of 20–70 well-behaved continuous GPS stations within 2000 km of Jamaica (representing the maximum interstation distance over which GPS noise remains strongly correlated, i.e. Marquez-Azua & DeMets 2003). For the 30 stations in Jamaica, the common-mode noise corrections reduces the magnitudes of the random and longer period noise in the station coordinate time-series by ∼20 per cent in both horizontal components relative to the unadjusted coordinate time-series. The corresponding changes in the GPS station velocities average only 0.05 and 0.15 mm yr^{-1} in the north and east velocity components, but range up to 0.7 and 1.1 mm yr^{-1} in the north and east velocity components at two campaign sites.

Table 2. GPS station information.

Site name	Coordinates		Station days														Velocity[a]	
	Latitude (N)	Longitude (E)	1998	1999	2000	2001	2002	2003	2004	2005	2006	2007	2008	2009	2010	2011	North	East
ALEX	18.31	−77.35	–	–	–	9	–	7	7	–	–	8	–	6	6	–	7.1 ± 0.4	4.0 ± 0.4
BOSC	18.40	−76.97	–	1	8	8	7	8	8	–	8	–	–	–	–	–	7.3 ± 0.4	4.0 ± 0.4
BRAE	17.95	−76.89	–	–	–	–	–	–	–	–	8	–	10	10	–	8	8.7 ± 0.9	7.1 ± 0.6
BTCC	18.40	−77.37	–	–	–	5	–	8	4	–	–	8	–	–	–	1	7.5 ± 0.4	4.0 ± 0.5
CASL	18.14	−76.36	–	–	3	7	8	13	14	–	–	8	–	7	–	–	7.7 ± 0.3	5.0 ± 0.4
CAVE	18.23	−77.37	–	–	–	7	–	10	8	5	9	–	–	–	9	–	6.8 ± 0.4	5.0 ± 0.4
DAVD	18.03	−76.79	–	–	–	–	–	–	–	–	–	77	30	–	–	–	7.4 ± 1.0	6.4 ± 1.3
DISC	18.46	−77.40	4	–	5	–	6	5	10	–	–	6	–	10	–	–	8.1 ± 0.4	4.2 ± 0.4
FONT	18.06	−77.94	–	2	4	4	9	11	7	–	–	–	–	–	–	7	6.6 ± 0.4	6.6 ± 0.4
HALS	17.93	−77.25	–	–	–	7	8	8	12	–	–	8	–	–	8	–	6.3 ± 0.5	7.2 ± 0.4
JAMA	17.94	−76.78	–	87	210	351	295	132	–	–	191	124	–	–	–	–	8.7 ± 0.5	4.7 ± 0.9
KEMP	17.86	−77.29	–	–	–	–	–	–	–	8	–	8	–	7	–	7	6.9 ± 0.8	10.0 ± 1.5
KNOX	18.15	−77.45	–	–	–	7	10	8	10	4	–	5	–	10	–	–	7.1 ± 0.5	5.7 ± 0.5
LINS	18.14	−77.03	–	–	–	–	–	–	150	210	45	73	22	206	97	–	7.6 ± 0.5	4.8 ± 0.5
LION	17.81	−77.24	–	–	–	–	–	–	–	172	154	57	–	–	16	–	7.9 ± 0.5	7.2 ± 0.5
MANC	18.05	−76.27	–	–	–	–	–	–	–	–	7	–	9	8	–	–	7.2 ± 0.8	6.5 ± 1.0
MAND	18.01	−77.50	–	2	3	5	8	12	8	–	–	7	–	–	9	–	7.0 ± 0.4	7.1 ± 0.4
MCAY	17.42	−75.97	–	–	–	–	–	–	–	–	–	9	–	–	9	–	7.4 ± 1.6	8.2 ± 2.8
MNRO	17.93	−77.69	–	–	–	–	–	–	–	–	8	–	8	13	–	9	7.6 ± 0.5	7.7 ± 0.6
MRNT	17.92	−76.18	–	–	5	1	8	11	10	–	7	–	–	8	10	–	7.4 ± 0.4	7.0 ± 0.4
MVRN	17.98	−77.72	–	–	1	–	–	–	–	–	–	–	11	–	–	10	6.5 ± 0.6	6.8 ± 1.0
NCAS	18.07	−76.71	–	–	5	6	7	8	11	–	5	10	–	–	7	–	6.9 ± 0.4	5.1 ± 0.4
NGLF	18.28	−78.32	–	2	3	4	4	12	12	–	–	9	–	–	8	–	6.3 ± 0.3	4.8 ± 0.3
NUTF	18.31	−76.83	–	–	1	–	–	–	–	–	–	–	10	–	–	8	6.8 ± 0.5	3.5 ± 1.0
PCJB	18.01	−76.79	–	–	8	13	8	8	8	–	8	–	–	7	–	–	7.6 ± 0.4	6.3 ± 0.4
PEDR	17.02	−77.78	–	–	–	–	–	–	–	7	–	8	–	8	–	–	7.0 ± 0.7	10.0 ± 0.9
PIKE	18.23	−77.53	–	–	6	11	316	313	142	38	107	–	320	276	365	139	7.5 ± 0.4	4.2 ± 0.4
PLND	17.74	−77.16	–	–	8	9	305	216	–	6	147	278	321	225	244	104	7.1 ± 0.4	7.9 ± 0.4
PYRA	18.49	−77.81	–	–	1	–	–	–	–	–	–	–	9	–	–	–	6.2 ± 0.8	3.3 ± 1.0
UWIN	18.00	−76.75	–	2	15	8	8	19	14	–	9	–	10	–	12	8	7.6 ± 0.4	5.6 ± 0.4

[a]Velocities are in millimetres per year. Standard errors for uncertainties are shown.

Each GPS site velocity was transformed from ITRF2008 to a Caribbean Plate reference frame (Fig. 3) by subtracting from each site velocity a velocity that is predicted at the site by the angular velocity for the Caribbean Plate relative to ITRF2008 (Table 2). We determined the angular velocity for the Caribbean Plate relative to ITRF2008 from the motions of 12 GPS sites on the Caribbean Plate, five located in the eastern Caribbean, one in southern Hispaniola and six in the western Caribbean and Central America. Both the angular velocity and its weighted rms misfit, 0.93 mm yr^{-1} in both the north and east velocity components, are close to those reported by DeMets *et al.* (2007) from an inversion of 15 velocities for Caribbean Plate sites. The ITRF2008 velocities of all sites used for the analysis were corrected assuming the motion of ITRF2008 relative to Earth's centre of mass is the same as that for ITRF2005, 0.3, 0.0 and 1.2 mm yr^{-1} in the X, Y and Z directions, respectively (Argus 2007). Given the small geographic extent of our study area, none of our results are sensitive to the geocentral translation correction that is applied to all of the GPS velocities in the analysis.

3.3 GPS velocities relative to the Caribbean Plate

Jamaica: Relative to the Caribbean Plate, all GPS sites in Jamaica move generally to the SW at rates that decrease from 7.3 ± 1.0 mm yr^{-1} at locations in northern Jamaica to 3.9 ± 0.8 mm yr^{-1} at locations in southern Jamaica (Fig. 3). Highly oblique convergent motion across the east–west-trending Gônave–Caribbean Plate boundary thus occurs, consistent with the velocities described previously by DWG07. The average southward component of motion of 2.6 ± 0.6 mm yr^{-1} is remarkably consistent everywhere on the island (Fig. 4b), in contrast to the decrease from 6.5±1.0 mm yr^{-1} along the island's north coast to 2.3±0.6 mm yr^{-1} along its southern coast in the magnitude of the west-directed component of motion (Fig. 4a). Consequently, GPS site directions rotate progressively CCW (counterclockwise or anticlockwise) between the north and south coasts of the island (Fig. 3).

The velocities of GPS sites of MCAY and PEDR, ∼50 and 80 km, south of the main island (Figs 3 and 4) reinforce the patterns described above. The southward velocity component at both sites agrees with the average 2.6 ± 0.6 mm yr^{-1} southward component of motion measured at all the Jamaican stations (Fig. 4b), possibly suggesting that south-directed convergence is accommodated within the northern Nicaragua Rise south of Jamaica. The west-directed velocity component at both sites agrees with the velocity gradient defined by the GPS sites on the main island (Fig. 4a) and differs insignificantly from zero at site PEDR ∼80 km south of the island. This suggests that all shear-related deformation occurs on plate boundary faults north of site PEDR.

The velocity gradients described above are even better displayed when site velocities are referenced to a station centrally located on the island (Fig. 3b). Relative to the continuous GPS station PIKE (Table 2), sites located north of the Plantain Garden fault and the central Jamaica fault system are either stationary or move no faster than ∼1–2 mm yr^{-1} to the SE (Fig. 3b). In contrast, sites located south of the central Jamaica fault system move to the ESE at rates that increase from 1 to 6 mm yr^{-1} southward from the central Jamaica fault system.

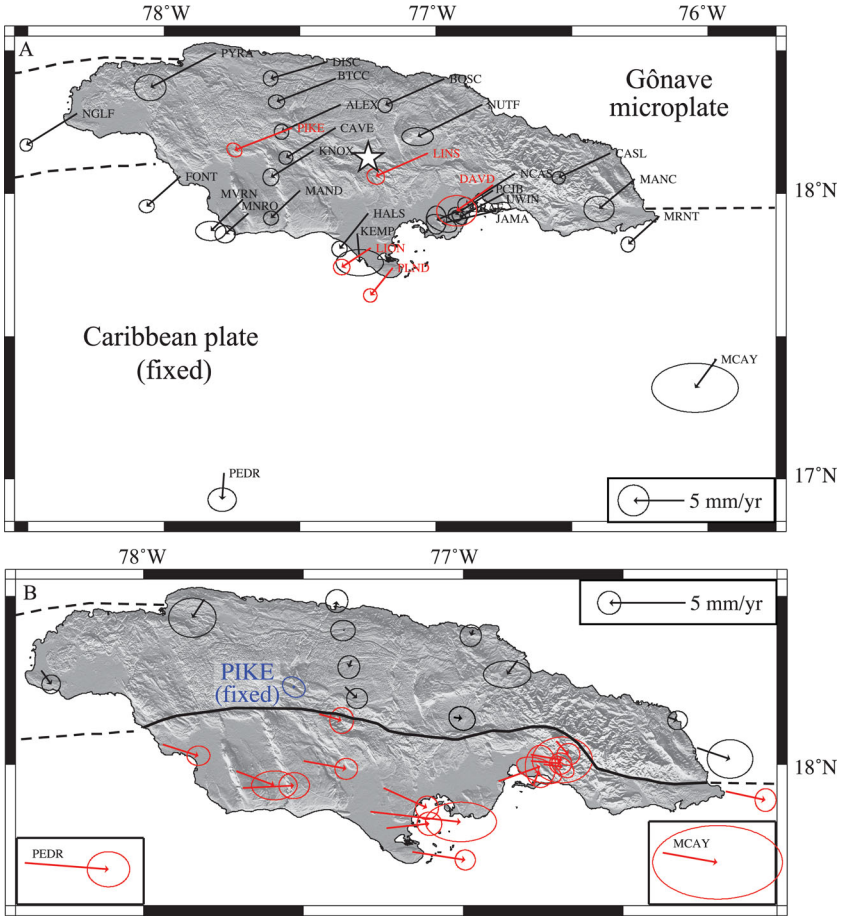

Figure 3. (a) Jamaica GPS site velocities relative to the Caribbean Plate, with one sigma, 2-D error ellipses. Continuous and campaign site velocities are shown in red and black, respectively. Star shows origin of N–S velocity transect in Fig. 4. Velocity scale is in lower right corner of the map. (b) Jamaica GPS site velocities relative to the campaign station PIKE. Velocities shown in black are north of the Plantain Garden fault and central Jamaica fault system, whereas velocities shown in red are south of these faults. Velocity scale is in upper right corner of the map. Both figures show 90-m Space Shuttle Topographic Radar Mission topography illuminated from the southwest.

Other locations: Fig. 5(a) shows velocities for the other 96 stations used in our analysis. The velocities of sites in Hispaniola are described and modelled by Calais *et al.* (2010); we reserve an in-depth analysis and discussion of those velocities for Benford *et al.* (In preparation, 2012a). Velocities from Puerto Rico and vicinity are also described and used by Benford *et al.* (In preparation, 2012a). We refer readers to Jansma & Mattioli (2005) for modelling and interpretation of earlier velocity fields for the Puerto Rico–Virgin Island region.

4 PLATE-BOUNDARY GEOMETRY AND FAULT SLIP RATES FROM BLOCK MODELLING

We next use the GPS velocities described above and shown in Fig. 5(a) to evaluate a series of models with differing assumptions about how faults in Jamaica transfer slip from the Plantain Garden fault of southeastern Jamaica to the Walton fault offshore of western Jamaica. Previous authors have variously proposed that slip is transferred by (1) left-lateral shear across a broad, east–west striking zone that crosses the island (Burke *et al.* 1980; Wadge & Dixon 1984), (2) two right-stepping restraining bends that connect the Plantain Garden and South Coast fault zone to the Duanvale fault (Mann *et al.* 1985) and (3) a series of CCW-rotating blocks bounded by the island's major E–W strike-slip faults (Draper 2008).

Following their lead, we first test different possible geometries and locations for an assumed discrete Gônave–Caribbean Plate boundary passing through the island (Fig. 6). We then test more complex models in which deformation on the island is characterized using one fault-bounded block (Fig. 7). Throughout the analysis, we use geological and seismic information to constrain the proposed fault and block geometries and use the model fits for rigorous comparisons of the alternative models. Although our GPS velocity field is too widely spaced to test Draper's (2008) concept of multiple rotating blocks on the island, we show below that the velocity field is well fit by a simpler, one-block model.

4.1 Model methods and assumptions

Our models were produced using Blocks software described by Meade & Loveless (2009), who apply linear spherical block theory to decompose interseismic GPS velocities ($\tilde{v}_{\rm I}$) into the rotation of fault-bounded blocks ($\tilde{v}_{\rm B}$), internal homogenous strain within the blocks ($\tilde{v}_{\varepsilon}$) and elastic strain accumulation on the faults ($\tilde{v}_{\rm E}$). This relationship can be expressed by:

$$\tilde{v}_{\rm I} = \tilde{v}_{\rm B} + \tilde{v}_{\varepsilon} + \tilde{v}_{\rm E}, \quad (1)$$

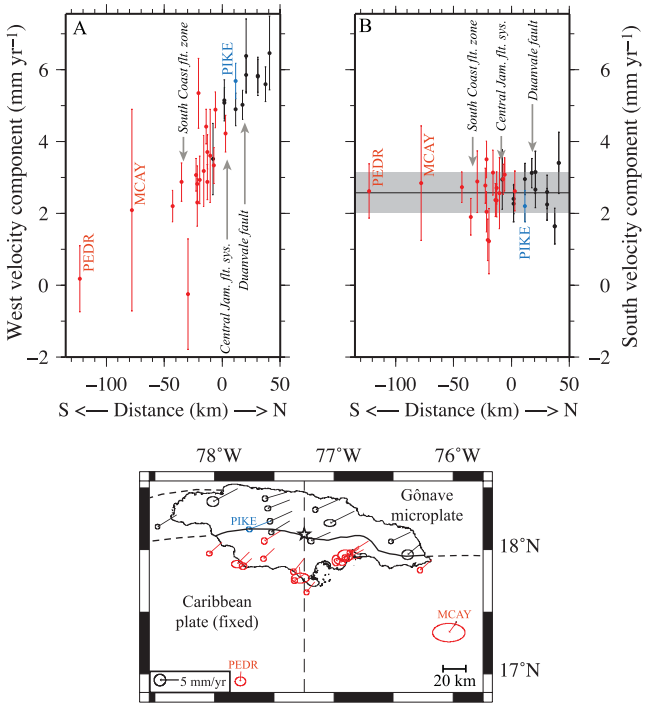

Figure 4. (a) West velocity component of GPS velocities from Fig. 3 versus distance along a N–S transect whose origin is shown by the star in the map beneath. (b) South velocity component of GPS velocities projected along the same transect. Grey shaded area is the 95 per cent confidence interval in the weighted mean velocity component. All rates are in a Caribbean Plate reference frame and are shown with their standard errors. GPS velocities from stations south of the Plantain Garden fault and central Jamaica fault system are shown in red. PEDR and MCAY indicate GPS velocities for stations on cays south of the main island of Jamaica (locations shown in the map beneath). Fault locations are shown in Fig. 2(a).

(from Meade & Loveless 2009, eq. 1). The rates and directions of fault slip predicted by a given block model are determined solely from the relative rotations of the adjacent blocks and fault geometry. These rotations, however, are estimated from an inversion of the observed interseismic velocities that simultaneously estimates the effects of the block rotations, internal homogeneous block strain and elastic strain from frictional locking of all the faults in the model. We do not estimate internal homogeneous strain of any of the blocks in our models, primarily because too few GPS sites are located on any likely block in Jamaica to estimate both its rotation and internal strain.

Three assumptions are required about faults for our modelling, as follows: their locking depths, their dips and the nature of frictional coupling across the faults. Wiggins-Grandison (2004) finds that relocated earthquakes in Jamaica occur primarily at depths between 10 and 22 km. Here, we assign a uniform fault-locking depth of 15 km. We also evaluated model results for locking depths as shallow as 10 km and as deep as 20 km, but determined that the estimated fault slip rates changed by only 10–15 per cent, within their estimated uncertainties. Strike-slip faults are assigned vertical dips; reverse faults are assigned dips of 60°, based on the known fault geometries of Jamaica, earthquake focal mechanisms and gravity modelling (e.g. Horsfield 1974; DeMets & Wiggins-Grandison 2007; Benford *et al.*, In preparation, 2012b).

For our modelling, we assume complete and uniform interseismic coupling across all block boundary faults, thereby maximizing the elastic deformation component in eq. (1). Consequently, the angular velocities that describe each block's motion are the only parameters estimated during each velocity field inversion. As described below, this simple model fits GPS velocities in Jamaica within their estimated uncertainties.

We impose a full interseismic fault-locking assumption for two reasons. First, only one GPS transect of Jamaica's E–W-striking faults has enough stations (77.4°–77.3°W in Fig. 3) to reliably estimate the local magnitude of interseismic coupling. Second, an inverse problem in which block rotations and fault coupling are estimated simultaneously may be poorly posed at deformation rates as slow as those in Jamaica because the sub-mm yr^{-1} differences between the velocity field gradients associated with fully or partially locked faults are smaller than the underlying GPS velocity uncertainties. At these slow rates, estimates of fault coupling and block rotations will trade-off strongly, guaranteeing that neither will be well determined. The assumption of full interseismic coupling is a limiting factor of our analysis and merits further investigation when more closely spaced, better-determined GPS site velocities become available.

An inversion of the GPS site velocities described above using Blocks gives as output an estimate of the angular velocity for each block in the model and the angular velocity uncertainties. Each GPS site is affiliated with a block in the model depending on the geometry of the faults that define the blocks; the estimated angular velocities therefore depend implicitly on the block geometry. The angular velocity of a given block also depends, to varying degrees, on the velocities of GPS sites exterior to its boundaries because of elastic deformation associated with locked faults along all the block boundaries.

4.2 Plate geometries and kinematic constraints

The boundaries of the North America Plate, the largest block in the model, are well known and are not varied in the models tested below. Similarly, the boundaries of the Caribbean Plate are well defined and not varied except along its boundary with the Gônave microplate in Jamaica. We use the MORVEL Caribbean–North America angular velocity [73.9° S, 32.6° E, 0.190° Myr^{-1}; DeMets *et al.* 2010] to tie the North America Plate to the Blocks model.

Although the northern, western and most of the southern boundaries of the Gônave microplate are well defined by the Oriente fault, Cayman spreading centre and Walton, Enriquillo and Plantain Garden faults (Fig. 1), the location of the eastern boundary of the Gônave microplate in Hispaniola is poorly defined. Specifically, the boundary could be located as far east as the Mona Passage between eastern Hispaniola and Puerto Rico (Fig. 5), as assumed by Manaker *et al.* (2008), or might be located in central or western Hispaniola (Mann *et al.* 1995, 2002). In a related paper, we use the same GPS velocities from the northern Caribbean to demonstrate that a Hispaniola block moves independently from the Gônave microplate and has a shared, likely diffuse boundary in western Hispaniola (Benford *et al.*, In preparation, 2012a). Hereafter, we use the Hispaniola block geometry preferred by Benford *et al.* (Fig. 5).

All our models include a North Hispaniola block bordered by the Septentrional fault to the south and the northern Hispaniola fault and Puerto Rico trench to the north (Fig. 5), consistent with the regional block configuration used by Manaker *et al.* (2008) and Calais *et al.* (2010).

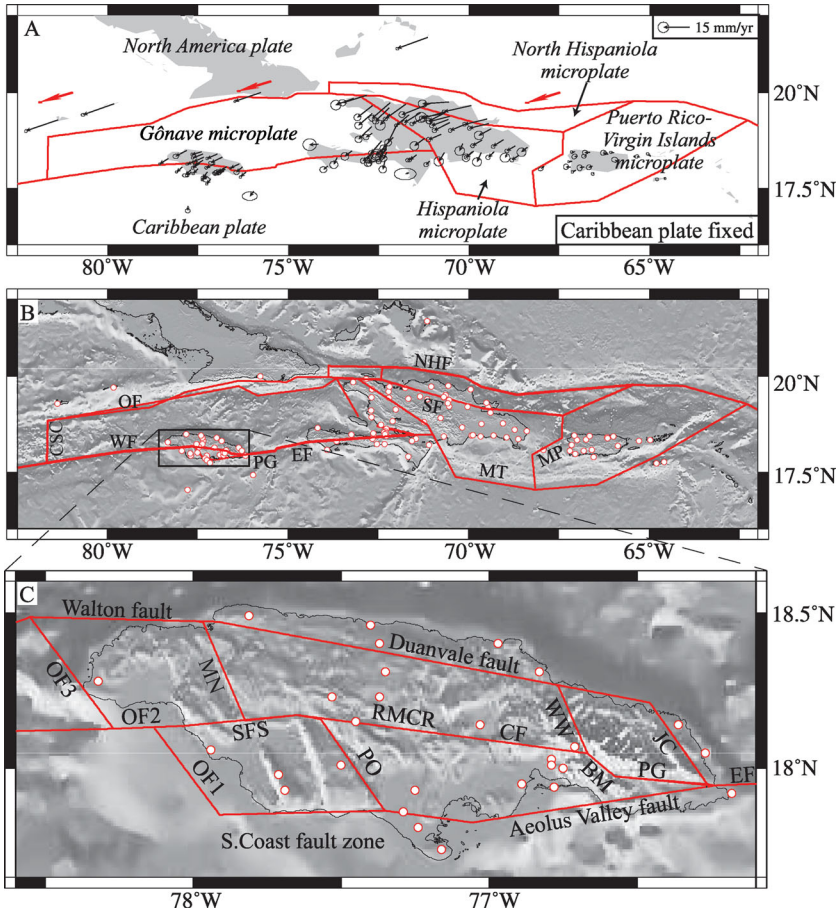

Figure 5. (a) Regional GPS velocities relative to Caribbean Plate. Velocities from Hispaniola are taken from Calais *et al.* (2010). Uncertainty ellipses are 2-D, one-sigma. Velocity scale is in upper right corner of the map. Red lines mark plate boundaries and major faults used for the analysis. Red arrows show North America Plate motion predicted by MORVEL. All plates and blocks included in the analysis are labelled. (b) Faults for northern Caribbean Plate boundary used in the analysis. GPS site locations are shown by red circles. Fault name abbreviations are: CSC, Cayman spreading centre; EF, Enriquillo fault; MP, Mona Passage; MT, Muertos trench; NHF, North Hispaniola fault; OF, Oriente fault; PG, Plantain Garden fault; SF, Septentrional fault and WF, Walton fault. (c) Simplified fault geometry of Jamaica used in the analysis. OF1, OF2 and OF3 refer to offshore faults 1, 2 and 3, respectively. Other fault name abbreviations are given in the caption to Fig. 2(a).

4.3 Comparisons of discrete boundary and block geometries

4.3.1 Methods

The goodness-of-fit for each assumed geometry for the Gônave–Caribbean Plate boundary in Jamaica is quantified using reduced chi-squared (χ^2_ν) from the Blocks inversion (Table 3), where χ^2_ν is the weighted, summed least-squares misfit χ^2 divided by the degrees of freedom in the model. Values of χ^2_ν that are smaller than 1 indicate that a model geometry fits the GPS velocities within their estimated uncertainties. Conversely, values of χ^2_ν greater than 1 indicate that the misfits exceed the estimated uncertainties. To better compare models and their fits to the subset of GPS site velocities of Jamaica, we calculate χ^2_ν for just the 30 sites in the Jsf3amaica archipelago (Table 3). The degrees of freedom are defined by the number of GPS velocity components that are inverted (126 velocities and 252 velocity components) to estimate all of our trial models reduced by the number of parameters that are adjusted to fit those velocities.

All the models we tested have either five plates (i.e. Caribbean, Gônave, Hispaniola, North Hispaniola and Puerto Rico–Virgin Islands) or six plates (including Jamaica) whose angular velocities are estimated. We use the Stein & Gordon (1984) F-ratio test to evaluate the improvements in fit of the more complex six-plate models relative to the five-plate models; the F-ratio test is well suited for this analysis given its inherent insensitivity to incompletely known data uncertainties. Best-fitting angular velocities and their uncertainties are given in Table 4 for plates directly relevant to this analysis (Jamaica, Gônave, Caribbean and North America). Angular velocities for other microplates included in this analysis (Hispaniola and Puerto Rico–Virgin Islands) are documented in Benford *et al.* (In preparation, 2012a).

4.3.2 Tests of discrete plate boundary geometries

We first tested geometries for the Gônave microplate boundary through Jamaica, assuming in each case that the plate boundary is defined by one or more faults that connect to form a continuous, discrete boundary. Each boundary follows the traces of known faults and is guided to some degree by earthquake epicentre locations (Figs 5 and 6). The geometry referred to as the northern discrete model, in which the Blue Mountains of eastern Jamaica form a large restraining bend that links the Plantain Garden fault of southeast Jamaica to the Duanvale fault of northern Jamaica (Fig. 6a)

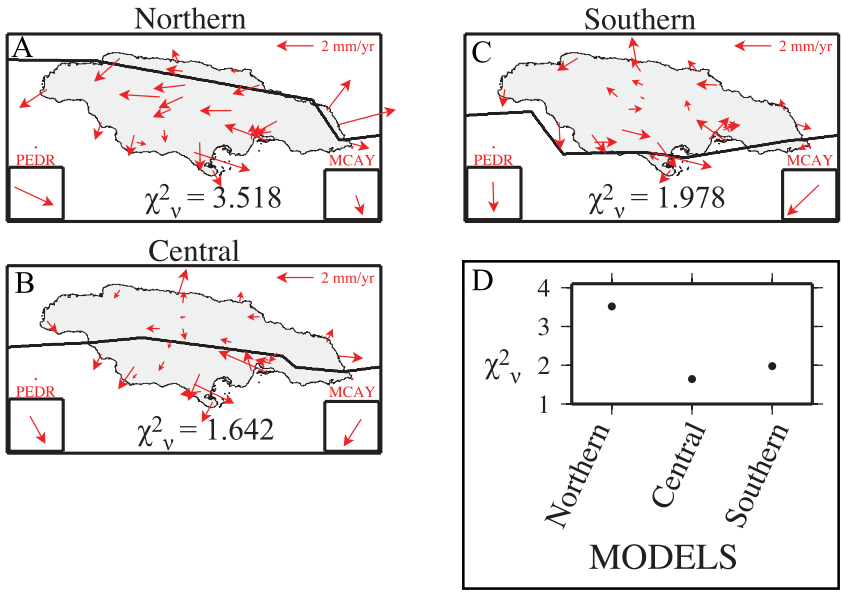

Figure 6. (a–c) Discrete-boundary models and their residual velocity fields, as described in text. Each assumed discrete-boundary is shown by the thick black line and is comprised of some subset of the faults shown in Fig. 5(c). Red arrows show the observed GPS site velocities from Fig. 3(a) reduced by the velocity predicted by its corresponding discrete-boundary model. Residual velocity scale is shown in upper right. Stations PEDR and MCAY from cays south of the main island (Fig. 3) are shown as insets. (d) Reduced chi-squared ($\chi^2{}_\nu$) for all three discrete-boundary models—lower values of $\chi^2{}_\nu$ correspond to improved fits.

fits the data more poorly than any discrete-boundary geometry we tested (including geometries not shown in Fig. 6). The combined weighted root-mean-square (WRMS) east and north velocity misfits of 1.4 mm yr^{-1} for the 30 Jamaica GPS sites (Table 3) for this geometry exceeds their estimated velocity uncertainties by a factor of 1.9 (i.e. $\sqrt{\chi^2_\nu} = \sqrt{3.5}$).

The central discrete geometry in which slip on the Plantain Garden fault is transferred to the central Jamaica fault system across a short segment of the Blue Mountain restraining bend (Fig. 6b) better fits the GPS velocities than the other discrete boundary geometries we tested (Fig. 6d), mainly because of improved fits to GPS velocities in central and northern Jamaica. The WRMS misfit for this geometry is 1.0 mm yr^{-1}, about 30 per cent larger than the average velocity uncertainty. The velocities of sites located north of the assumed boundary are well fit for this geometry (Fig. 6b). South of the assumed boundary, 8 of the 10 stations that are located 20 km or more south of the assumed boundary have southwest-directed residual motions of 0.5–2.2 mm yr^{-1}, including the two GPS sites at Pedro and Morant Cays south of the main island.

Finally, we tested a southern discrete geometry in which slip on the Plantain Garden fault is transferred by the Aeolus Valley fault to the South Coast fault zone and is then transferred northward to the offshore Walton fault across an assumed restraining bend along the southwest coast of Jamaica (Fig. 6c). Although, the WRMS misfit for this geometry is only about 15 per cent larger than for an assumed discrete boundary in central Jamaica (Fig. 6b), site velocities in the northern half of the island are fit more poorly for an assumed boundary in southern Jamaica.

We also tested other more complex discrete boundary geometries assuming different locations for the restraining bend in Jamaica. None, however, improved the fit relative to the central discrete geometry in which Gônave–Caribbean Plate motion is assumed to follow a narrow boundary in central Jamaica (Fig. 6b). The best discrete boundary geometry thus misfits the GPS velocities at a level ∼30 per cent larger than the estimated velocity uncertainties, and moreover leads to a systematic southwest-directed residual velocity field in southern Jamaica and south of the island. We, thus, reject the hypothesis that the plate boundary is narrow and test more complex geometries in the following section.

4.3.3 Tests of more complex plate boundary geometries

Each of the more complex plate boundary geometries we tested includes a single fault-bounded block that is sandwiched between the Gônave microplate and Caribbean Plate (Fig. 7). We tested eight geologically plausible block models, each with three additional degrees of freedom relative to the discrete boundary models described above. Six of the eight block models improved the fit relative to the best discrete boundary model at the 99 per cent or better confidence level (Table 3).

Two models failed to significantly improve the fit, one that includes a block defined by the major faults that bound the topographically high and seismically active Blue Mountains of eastern Jamaica (Fig. 7b), and the other includes a block bounded by the Duanvale fault and the central Jamaica fault system (Fig. 7d). The former model fits the data worse than any other block model ($\chi^2_\nu = 2.9$), consistent with the poor fit of the analogous discrete-boundary geometry (Fig. 6a). The motion of the block is constrained solely by stations along its edges, making this a weak test for a Blue Mountain block. The latter model, shown in Fig. 7(d), reinforces the poor fit we found for the northern discrete boundary model (Fig. 6a). These argue against significant slip along the Duanvale fault of central Jamaica, where our GPS network crosses the fault as part of a N–S transect of the island (Figs 2b and 3).

One of the two best-fitting block fault models defines an elongate southern block bounded by the central Jamaica fault system and South Coast fault zone (Fig. 7e). This model fits the GPS velocities better than all three discrete boundary models (Fig. 6b) with a WRMS misfit (0.9 mm yr^{-1}) that is only 15 per cent larger than

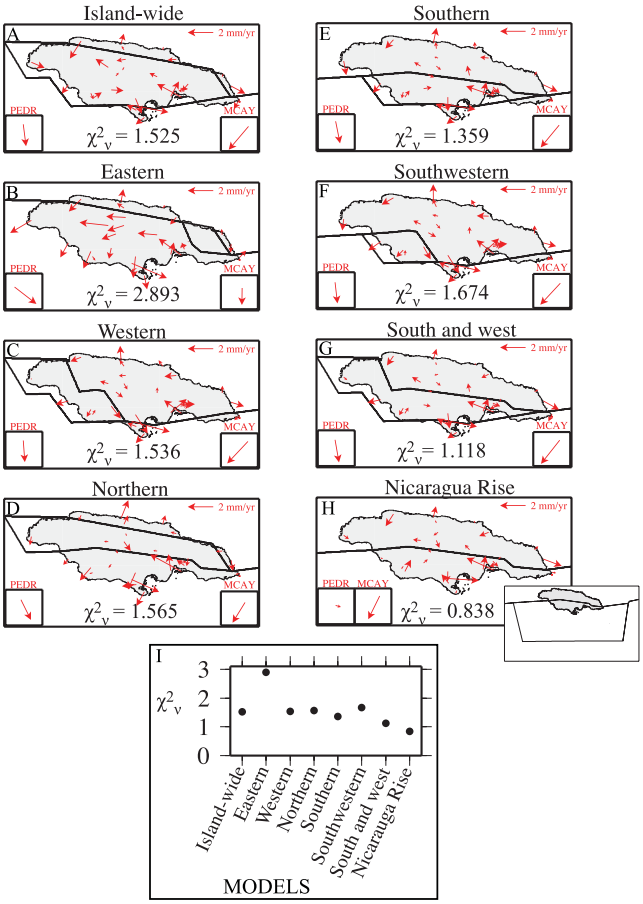

Figure 7. (a–h) Fits of candidate block models for deformation in Jamaica, as described in text. Block boundaries are shown by black lines and are comprised of subsets of the faults shown in Fig. 5(c). Red arrows show the observed GPS site velocities from Fig. 3(a) reduced by the velocity predicted by its corresponding block model. Residual velocity scale is shown in upper right. Stations PEDR and MCAY from cays south of the main island of Jamaica (Fig. 3) are shown as insets. Inset in (h) shows block geometry of Nicaragua Rise model. (i) Reduced chi-squared ($\chi^2{}_\nu$) for all eight block models—lower values of $\chi^2{}_\nu$ correspond to improved fits.

the estimated velocity uncertainties. Reflecting this good fit, the southern block model fits the GPS velocities everywhere on the island. Significant misfits of this model to the GPS velocities at Morant and Pedro Cays ∼50–80 km south and southeast of the main island (Fig. 6e) are similar to those for all but one of the block models and are treated below.

Given the success of the southern block geometry, we examined whether two plausible variations on the assumed southern block geometry would further improve the fit (Figs 7f and g). A geometry in which the eastern restraining bend is assumed to coincide with the Porus fault of south–central Jamaica, which is mapped but not named on the 1992 Jamaica Mining and Commerce structure maps, instead of the Blue Mountain restraining bend in eastern Jamaica (Fig. 7f) degrades the fit and is thus rejected. A model in which motion along the central Jamaica fault system is assumed to step northward to the Walton fault along the Montpelier-Newmarket fault zone of northwestern Jamaica (Fig. 7g) improves the fit and has an average velocity misfit equal to the average estimated uncertainty. This model predicts 4.6 ± 1.0 mm yr^{-1} of left-lateral motion on the Montpelier-Newmarket zone of western Jamaica. Given the absence of major throughgoing strike-slip faults in this area, we are sceptical of this model. Nonetheless, given the sparse distribution of GPS stations in northwestern Jamaica, more stations are needed for a stronger test of this and other geometries in which faults in northwestern areas of the island transfer slip northward off the central Jamaica fault system.

Finally, given that 2–3 mm yr^{-1} of southward motion is measured everywhere in Jamaica, including its southern cays (Fig. 4b), and that none of the discrete or block models described above fit the velocities at the cays (Figs 6 and 7a–g), we constructed a model in which Pedro and Morant cays are assumed to lie on the same block as much of southern Jamaica (inset to Fig. 7h). In effect, this model tests whether deformation can be partitioned into largely E–W shear on Jamaica and southward convergence south of the main island and cays.

The model described above (Fig. 7h) fits the velocities better than any of the previous discrete or block models, with χ^2_ν of 0.84 and combined WRMS of 0.7 mm yr^{-1} (Fig. 7i). The average velocity misfit is thus only 90 per cent of the estimated velocity uncertainties, making this model unique amongst the many models we tested. Although, deformation south of the island is almost surely accommodated by multiple faults over a wide area within the Nicaragua Rise, the good fit of our simplified geometry is encouraging. Given its superior fit, we adopt this hereafter as our preferred model and in Table 4 give the angular velocities that fully specify this model. Further discussion of the block motions and fault slip predicted by this model is found in the next section.

To determine whether the more complex single-block model is warranted by the improvement in fit, we compared the fits of the best discrete boundary model (Fig. 6d) and both the southern block geometry (Fig. 7e) and Nicaragua Rise block geometry (Fig. 7h). Using the Stein & Gordon (1984) F-ratio test for an additional plate and least-squares misfits $\chi^2 = 375.5$ for the best discrete boundary model and $\chi^2 = 300.1$ for the Nicaragua Rise block geometry (Fig. 7h), the value for F is 19.6. For comparison, the 99 per cent threshold for a significant improvement in fit for 3 versus 234 degrees of freedom is $F = 3.87$. The probability that random errors in the GPS velocities could result in this F-value is only 2 parts in 10^{11}. The additional block is thus warranted at much greater than the 99 per cent confidence level. Repeating the calculations for the southern block geometry (Fig. 7e) gives $F = 9.7$ ($\chi^2 = 333.9$ for this geometry; Table 3). The improvement in fit is also significant at a high confidence level, with a probability of only 5 parts in 10^6 that random errors in the GPS velocities could result in this F-value.

5 DISCUSSION

5.1 GPS velocity field interpretation

Independent of any modelling, the gradient in the Jamaica GPS velocity field along a N–S transect of the island (Fig. 3b) strongly indicates that one or more active plate boundary faults are located on the island. In particular, relative to a fixed GPS site (PIKE) near the centre of the island, all sites in Jamaica north of the central Jamaica fault system move only 1 mm yr^{-1} or slower, consistent with little or possibly no deformation in much of the northern half of the island. In particular, four stations that comprise a N–S transect of the Duanvale fault near 77.4°W show no evidence for active slip across that fault. Similarly, GPS site NGLF in western Jamaica and north of the central Jamaica fault system moves with the same velocity (within uncertainties) as GPS site CASL on the east coast of Jamaica (Fig. 3 and Table 2). By implication, little or no

Table 3. Parameters and results for models tested in Figs 6 and 7.

	Model	# of plates and microplates[a]	χ^2	χ^2 all 126 sites	χ^2 for 30 Jamaica GPS sites	WRMS (east) in mm yr^{-1} All sites	WRMS (north) in mm yr^{-1} All sites	WRMS (east) in mm yr^{-1} Jamaica	WRMS (north) in mm yr^{-1} Jamaica	Significance for improved fit (per cent)[b]
Discrete	Northern	5	584.6	2.47	3.52	1.27	1.07	1.14	0.80	–
	Central	5	375.5	1.59	1.64	0.90	0.97	0.60	0.77	–
	Southern	5	375.7	1.59	1.98	0.90	0.97	0.75	0.83	–
Plate/microplate	Island-wide	6	341.2	1.46	1.53	0.89	0.90	0.70	0.65	>99.9 per cent
	Eastern	6	502.5	2.15	2.89	1.15	1.02	0.90	0.81	Fit is worse
	Western	6	341.8	1.46	1.54	0.87	0.91	0.67	0.69	>99.9 per cent
	Northern	6	359.5	1.54	1.57	0.87	0.95	0.54	0.76	>98 per cent
	Southern	6	333.9	1.43	1.36	0.84	0.92	0.56	0.69	>99.9 per cent
	Southwestern	6	351.0	1.50	1.67	0.86	0.94	0.64	0.76	>99 per cent
	South and west	6	319.3	1.37	1.12	0.85	0.87	0.58	0.57	>99.9 per cent
	Nicaragua Rise	6	300.1	1.28	0.84	0.82	0.85	0.50	0.51	>99.9 per cent

[a]Angular velocities are estimated for the Caribbean Plate, Gônave, Hispaniola, North Hispaniola, Puerto Rico–Virgin Islands and sometimes Jamaica microplates. The North America Plate angular velocity is included in the model, but is constrained and thus excluded from the plate/microplate count.
[b]Significance is calculated using the Stein & Gordon (1984) F-ratio test for an additional plate and three additional degrees of freedom. Plate/microplate models are compared to the best-fitting discrete model—the central discrete model.

east-to-west contraction appears to occur across the northern half of the island.

All of the GPS sites on the southern half of the island move significantly relative to PIKE, with velocities increasing to the south to rates as fast as 6 mm yr^{-1} to the east (Figs 3 and 4). To first order, the velocities are consistent with strike-slip motion on the central Jamaica fault system, on the South Coast fault zone or on both.

All Jamaica GPS sites move 2.6 ± 0.6 mm yr^{-1} southward towards the Caribbean Plate interior (Fig. 4b), including the two sites located 50 and 80 km south of the island. The consistent southward motion may indicate that ∼N–S contraction may occur in the northern Nicaragua Rise south of Jamaica. Some evidence supports this explanation—one of the two largest earthquakes in or near Jamaica in the past 70 yr was the $M_o = 6.9$ 1941 April 7 earthquake ∼80 km southwest of the island within the Nicaragua Rise (Event #1 in Fig. 2c; Van Dusen & Doser 2000). The *P*-axis for this strike-slip earthquake is oriented NNE–SSW, consistent with approximate N–S contraction across the Nicaragua Rise. Alternatively, the slow southward motions of all the network sites could be an artefact of a ∼2 mm yr^{-1} systematic bias in the plate velocities predicted by the Caribbean Plate angular velocity near Jamaica. We consider this less likely because the Caribbean Plate angular velocity estimate is relatively robust with respect to the subset of site velocities that are used to estimate it (DeMets *et al.* 2007).

5.2 Model implications and limitations

5.2.1 Discrete versus distributed plate boundary in Jamaica

A key goal of our work was to test whether GPS velocities from Jamaica are more consistent with a geometry in which a discrete plate boundary passes through the island or with plate boundary geometries that incorporate an independently moving block between the Gônave and Caribbean plates. The highly significant improvements in the fits of both the southern block and Nicaragua Rise block geometries (Figs 8a and b) relative to the fit for the best-fitting discrete boundary geometry (Fig. 6b) argue against the simpler discrete boundary assumption. Instead, 7 ± 1 mm yr^{-1} of WSW–ENE motion between the Gônave and Caribbean plates (Figs 8a and b) is accommodated across the boundaries of a block whose northern and southern boundaries are defined respectively by the central Jamaica fault system and unknown faults within or near southern Jamaica (Fig. 8a) or in the northern Nicaragua Rise (Fig. 8b).

Seismic and geological observations reinforce the kinematic evidence against the simpler discrete-boundary model. Seismicity in Jamaica is widespread (Figs 2c and 8), contrary to the presumption of concentrated deformation inherent in a discrete-boundary model. Numerous earthquakes in the Blue Mountains of eastern Jamaica (Figs 2c and 8) and active anticlines (i.e. Long and Dallas Mountains in northeast Kingston) at the western edge of the Blue Mountains (Draper 2008) argue strongly for the existence of such a restraining bend. However, neither of the discrete-boundary models that include restraining bends solely in eastern Jamaica (Figs 6a and b) fits the GPS velocities well.

5.2.2 Preferred and alternative block geometries

Two-block geometries, shown in Figs 8a and b, fit the GPS velocities close to or within their estimated uncertainties. For several reasons, we prefer the geometry that assumes deformation extends south of the island on as-yet unidentified faults within the Nicaragua Rise (Fig. 8b). Foremost, this geometry fits the velocities ∼20 per cent better than the alternative geometry. Moreover, the Blocks velocity inversion that employs this geometry cleanly partitions deformation in the study area into left-lateral strike-slip motion along the WNW-trending central Jamaica fault system and N–S convergence across submarine structures south of Jamaica, in accord with the geological and seismic evidence for shear-dominated deformation on the island. Finally, the elastic component (red arrows in Fig. 8c) of the GPS velocities predicted by Blocks for the preferred geometry parallels Jamaica's strike-slip faults everywhere on the island, in accord with elastic deformation observed in many strike-slip settings worldwide (e.g. Genrich *et al.* 2000; Pearson *et al.* 2000; Spinler *et al.* 2010).

Using the alternative geometry (Fig. 8a), the Blocks model predicts 4–5 mm yr^{-1} of N–S convergence across the South Coast fault zone of southern Jamaica, inconsistent with the geology and topography of this apparent strike-slip fault zone.

Table 4. Angular velocities from Blocks software inversion using the geometry shown in Fig. 7(h).

Plate pair	Angular velocity[a]			Ellipse axes		Azimuth of major axis	Rotation uncertainty	Variances (σ_{xx}, σ_{yy}, σ_{zz}) and covariances (σ_{xy}, σ_{xz}, σ_{yz})[b] 10^{-8} radians^2/Myr^2					
	Latitude	Longitude	ω	Major	Minor			σ_{xx}	σ_{xy}	σ_{xz}	σ_{yy}	σ_{yz}	σ_{zz}
	°N	°E	° Myr^{-1}	°	°		° Myr^{-1}						
CA-ITRF08[c]	37.3	−100.6	0.247	2.9	0.9	302.83	0.013	0.79	−1.75	0.50	6.04	−1.81	0.76
CA-ITRF08[d]	37.7	−101.0	0.243	2.9	0.9	302.83	0.013	0.79	−1.75	0.50	6.04	−1.81	0.76
GV-CA	−24.5	100.1	0.526	1.4	0.6	26.32	0.069	7.64	−30.35	10.17	127.67	−42.53	14.51
GV-NA	−4.1	106.5	0.473	2.9	0.6	9.77	0.065	7.69	−28.80	9.87	114.94	−39.34	13.58
JA-CA	16.6	−75.5	0.765	0.8	0.4	306.58	0.194	51.34	−224.18	74.28	988.17	−327.21	108.73
JA-GV	19.8	−77.2	1.287	0.5	0.4	353.41	0.212	63.08	−270.51	89.70	1179.40	−390.68	129.84

[a]Angular velocities describe counter-clockwise rotation of the first plate/block relative to the second plate. Ellipse axes are semi-major and semi-minor. Plate abbreviations: CA, Caribbean; JA, Nicaragua Rise (Jamaica); GV, Gônave and NA, North America.
[b]Covariances are Cartesian and propagated from data uncertainties. Elements σ_{xx}, σ_{yy} and σ_{zz} are the variances of the (0°N, 0°E), (0°N, 90°E) and 90°N components of the angular velocity.
[c]Derived assuming no motion relative to Earth's centre of mass.
[d]Derived from an inversion of 12 Caribbean Plate GPS site velocities corrected for assumed motions of $V_x = 0.3$, $V_y = 0.0$ and $V_z = 1.2$ mm yr^{-1} for ITRF2008 relative to Earth's centre of mass. The assumed motions are the same as for ITRF2005 relative to Earth's centre of mass (Argus 2007).

For the preferred geometry, the Caribbean–Gônave Plate angular velocity (Table 4) predicts 6–7 mm yr^{-1} of left-lateral slip between the two plates east and west of Jamaica (Fig. 8b). This motion is partitioned into ∼4–5 mm yr^{-1} of left-lateral, fault-parallel slip along the Plantain Garden fault and central Jamaica fault system (Fig. 8b) and 2.4 ± 1 mm yr^{-1} of N–S convergence across the hypothetical block boundary south of Jamaica (Fig. 8b).

One weakness of the preferred model is the absence of compelling seismic or marine geophysical evidence for active deformation within the Nicaragua Rise south of Jamaica. We are unsurprised that deformation in this area has gone unrecognized given the slow predicted deformation rate, the absence of high-resolution marine surveys in this area and the possibility that multiple faults within a diffuse deformation zone accommodate the convergence. A second shortcoming of the new model is that the current resolution of the GPS and seismic data put most of the seismic hazard on the Plantain Garden fault, active faults in the Blue Mountain restraining bend and the central Jamaica fault system. We assess the possible seismic hazard for the Kingston area in Section 5.2.4 based on this model. We consider it unlikely that all motion occurs on this series of faults based on recent work by Benford *et al.* (In preparation, 2012b); however, stronger tests for active deformation on faults other than those listed above will require more widely distributed GPS sites and better determined site velocities.

5.2.3 Implications for specific fault zones

We next describe briefly the implications of the preferred (Fig. 8b) and other models (Figs 6 and 7) for several prominent fault zones in Jamaica, namely, the Blue Mountains restraining bend of eastern Jamaica, the central Jamaica fault system, the South Coast fault zone and its postulated eastern continuation the Aeolus Valley fault and the faults in northern and eastern Jamaica, where little deformation appears to occur. Because the formal velocity uncertainties estimated by the Blocks software are based on the assumption that the fault-locking depths and block geometries are perfectly known, neither of which is true for our analysis, the formal uncertainties are surely too small. Numerical experiments suggest that the true uncertainties may be a factor of 2–3 times larger than the formal uncertainties. Uncertainties stated below represent our best estimate for a given rate.

Blue Mountains and a restraining bend in eastern Jamaica: Although, we approximate the Blue Mountain restraining bend of eastern Jamaica as a single fault at the western edge of the Blue Mountains, the widespread seismicity associated with this restraining bend (shown in Figs 8a and b) instead suggests that 2.6–4.0 mm yr^{-1} of predicted contraction (Figs 8a and b) is accommodated by multiple structures, possibly including the Blue Mountain fault, the Yallahs faults (Mann & Burke 1990) and actively growing anticlines in the capital Kingston (Draper 2008). Although, the topographically prominent John Crow Mountains of far eastern Jamaica (JC in Figs 2a and 5c) may accommodate some restraining bend deformation, none of the discrete-boundary or block geometries that include the John Crow Mountains as a block boundary adequately fit the GPS velocity field (e.g. Figs 7a, b and d). Discrete boundary and block geometries that extend the Blue Mountain restraining bend farther north along the Wagwater Belt (fault WW in Figs 2a and 5c and geometries shown in Figs 6a and 7b) also fit the velocities poorly, consistent with the northward

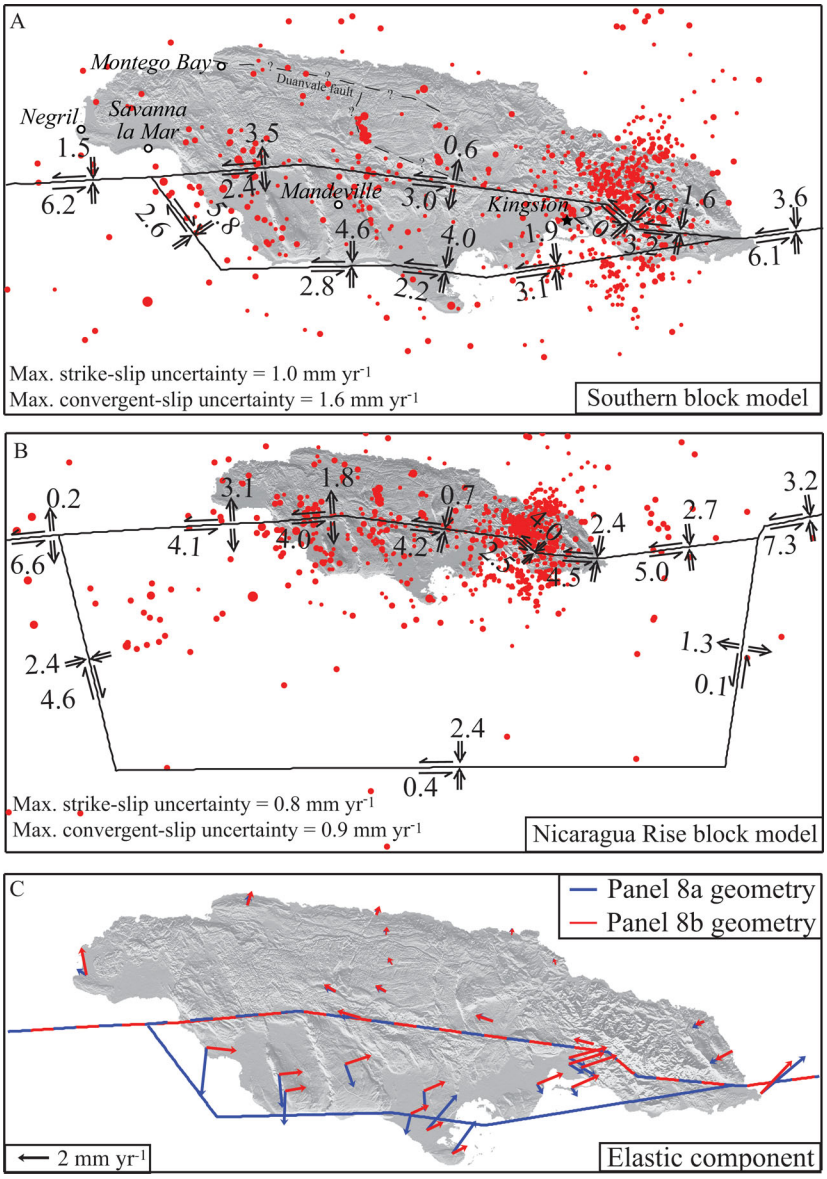

Figure 8. Slip rates predicted by the southern block model (Panel a) and the Nicaragua Rise block model (Panel b). All slip rates are in mm yr^{-1} and are specified as boundary-parallel and boundary-normal components for each fault segment. Red circles show ISC seismicity from Fig. 2. Slip rate estimates along the Blue Mountains fault are 2.0 mm yr^{-1} of left-lateral motion and 2.6 mm yr^{-1} of convergence for Panel (a) and 2.5 mm yr^{-1} of left-lateral motion and 4.0 mm yr^{-1} of convergence The dashed line in Panel (a) marks both the Duanvale fault and a zone where motion may be transferred to it from the central Jamaica fault system. (c) Elastic component of the modelled GPS velocities (blue arrows) for the southern block model shown in Panel (a) and the Nicaragua Rise model shown in Panel (b) (red arrows). Red-blue dashed line shows the northern block boundary assumed for both geometries. Velocity scale is in the lower left corner.

decrease in both the seismicity and topography associated with the Blue Mountain restraining bend (Fig. 8b).

Central Jamaica fault system and South Coast fault zone: Estimates of present slip rates along the central Jamaica fault system range from 2.4 to 4.2 mm yr^{-1} of left-lateral strike-slip in central Jamaica (Figs 8a and b), depending on which block geometry is employed. Slip of 4.2 $\pm$ 1 mm yr^{-1} is predicted in central Jamaica by our preferred model (Fig. 8b), whereas the South Coast fault zone is assumed to accommodate negligible or no slip. In contrast, the southern block model (Fig. 8a) partitions Gônave–Caribbean Plate slip nearly evenly between the South Coast fault zone (2.2–2.8 mm yr^{-1}), and the central Jamaica fault system (2.4–3.0 mm yr^{-1}), with negligible deformation assumed within the Nicaragua Rise south of Jamaica. Reasonable bounds for slip rates along both fault systems are 2–4 mm yr^{-1}, depending on the assumed block geometry (Figs 8a and b).

Aeolus Valley fault: The southern block geometry requires that some motion on the Plantain Garden fault be transferred southwestward to the South Coast fault zone (Fig. 8a) by one or more faults onshore and south of Jamaica. The Aeolus Valley fault, which intersects the eastern Plantain Garden fault (Fig. 2a), may be the best candidate for transferring this slip. The southern block model predicts that Caribbean–Gônave Plate motion is partitioned nearly evenly between the Aeolus Valley fault and western Plantain Garden

fault, such that each fault accommodates ∼3–5 mm yr^{-1} of oblique slip motion (Fig. 8b).

Duanvale fault and northern Jamaica: Although previous authors have hypothesized that the Duanvale fault plays an important role in Jamaica's tectonics (Mann *et al.* 1985; Mann *et al.* 2007; Draper 2008), none of the geometries that include the Duanvale fault give an acceptable fit to the GPS velocity field (Figs 6a, 7a and b). Combined with an absence of seismicity along much of the fault, we infer that at least the eastern segment of the Duanvale fault is inactive or slips too slowly to detect with GPS. Significant slip, however, may still occur along the Duanvale fault in northwestern Jamaica, where only one GPS station is located (site PYRA in Fig. 3). In this region, several small earthquakes along the Duanvale fault just east of Montego Bay (Fig. 8b) indicate that the fault is still active. A $M_w = 4.5$ left-lateral oblique slip earthquake that occurred in 2005 in central Jamaica north of the central Jamaica fault system (Fig. 2c, event #48) may indicate that some slip on the central Jamaica fault system is transferred north to the western portion of the Duanvale fault. Additional GPS sites in northwest Jamaica are needed to determine whether the fault is active in this region.

Walton fault: SeaMARC II side-scan mapping off the coast of western Jamaica identifies multiple active strands of the Walton fault, one at the same latitude (Fault E) as the central Jamaica fault system (Tyburski 1992). Modelling of our GPS velocities suggests that significantly more slip occurs along the central Jamaica fault system, east of Fault E, rather than along the Duanvale fault of northern Jamaica. Some slip along the central Jamaica fault system may thus continue westward to Fault E instead of stepping north to the Duanvale fault. If correct, this implies a smaller right-stepping restraining bend than postulated by previous authors, who instead envision much of the island as a restraining bend (Burke *et al.* 1980; Wadge & Dixon 1984; Mann *et al.* 1985; Draper 2008).

5.2.4 Implications for seismic hazard

Elastic strain accumulation appears to be highest in eastern Jamaica, where deformation is localized along the Plantain Garden and Aeolus Valley faults. Consistent with the conclusions of DWG07, our results imply high seismic risk for the capital city Kingston and its surrounding suburbs, which are the most densely populated areas on the island (Fig. 2a). Using plausible assumptions for the maximum rupture length of a future earthquake in eastern Jamaica (∼150 km), our modelling results indicate that enough elastic strain has accumulated since the destructive 1907 earthquake in eastern Jamaica to generate a $M_w \cong 7$–7.5 earthquake.

5.2.5 Model limitations and uncertainties

The slow deformation rates on the island (<7 mm yr^{-1}) and heterogeneous distribution of the GPS sites limit our ability to resolve deformation in more detail, even given the small uncertainties in our site velocities. For example, although east–west contraction likely occurs across the Santa Cruz and Don Figuerero Mountains in the interior of the southern block, we are unable to resolve any E–W contraction within this block given the slow deformation rates. Most of what we know about where fault slip extends offshore in western Jamaica is based on the velocities of just three GPS sites (PYRA, NGLF and FONT in Fig. 3a). Although these sites suggest that most and possibly all motion exits the island south of site NGLF, presumably on the central Jamaica fault system, better site coverage is needed to determine whether some fault slip may be transferred northward from the central Jamaica fault system to the Duanvale fault near the densely populated tourist area of Montego Bay (Figs 2a and 8a).

Because of the limited number of GPS sites, we largely limited our exploration of alternative block models to those with a single block. Given that the best-fitting block geometry (Fig. 8b) reduces the data variance by 98.3 per cent and has a WRMS misfit of only 0.7 mm yr^{-1}, our approach seems warranted. As a test, we subdivided the Jamaica block in our preferred geometry (Fig. 8b) into two blocks, one consisting of the elongate block in southern Jamaica (Fig. 8a) and the other extending southward from the South Coast fault zone into the Nicaragua Rise. Inverting the GPS velocities with this more complex geometry failed to improve the fit significantly and moreover predicted insignificant slip along the South Coast fault. A more complex block model awaits better-determined velocities at the present sites and new measurements in other areas of the island.

6 CONCLUSION

Relative to the Caribbean Plate, all GPS sites in Jamaica move generally to the SW at rates that decrease from 7.3 ± 1.0 mm yr^{-1} at locations in northern Jamaica to 3.9 ± 0.8 mm yr^{-1} at locations in southern Jamaica. GPS sites located north of the central Jamaica fault system have differential movements that are typically 1 mm yr^{-1} or less, consistent with little or possibly no deformation in much of the northern half of the island. In contrast, a well-defined GPS velocity gradient in central and southern Jamaica indicates that elastic deformation is concentrated across one or more faults in these areas of the island or south of the island.

Modelling of GPS velocities from Jamaica and adjacent islands for a series of candidate geometries for the Gônave–Caribbean Plate boundary yields two best-fitting geometries, one that assigns most of southern Jamaica to an independently moving block and another that partitions strike-slip motion along the Plantain Garden fault and central Jamaica fault system and southward convergence in the Nicaragua Rise. Both models improve the fit to the velocity field at better than the 99 per cent confidence level relative to a best-fitting discrete-boundary geometry and one fits the velocities within the estimated uncertainties. Both models partition 7 ± 1 mm yr^{-1} of Gônave–Caribbean Plate boundary motion between the central Jamaica fault system and faults farther south. Both moreover predict 3–4 ± 1 mm yr^{-1} of convergence across the seismically active Blue Mountain restraining bend of eastern Jamaica, adjacent to the densely populated capital city of Kingston.

None of the models that postulate significant slip along the prominent Duanvale fault of northern Jamaica adequately fit the GPS velocity field. In particular, slip faster than 1 mm yr^{-1} seems unlikely along the eastern half of the Duanvale fault. Almost no GPS velocities constrain our results along the western half of the Duanvale fault, where the fault passes near the densely populated tourist area of Montego Bay. Seismic hazard in northwestern Jamaica is thus still more poorly defined than elsewhere on the island.

ACKNOWLEDGMENTS

None of this work would have been possible without more than a decade of dedicated support from the Jamaica Earthquake Unit of the University of West Indies. We thank Gregory Peake of Spatial Innovision in Kingston and the Jamaican National Land Agency for

continuous data used in our analysis, and Glendon Newsome and Dr. Raymond Wright for their support and data. We thank the Jamaica Coast Guard, for sea transport to Morant and Pedro Cays and Dr. Byron Wilson for sea transport to the Hellshire Hills GPS site. We thank Jack Loveless for patient advice on the use of his Blocks software and constructive comments as a reviewer, and further thank Glen Mattioli for his in-depth, constructive review. This project was funded by National Science Foundation grant EAR-0609578. Some of this material is based on data provided by the UNAVCO Facility with support from the National Science Foundation (NSF) and National Aeronautics and Space Administration (NASA) under NSF Cooperative Agreement No. EAR-0735156. Figures were produced using Generic Mapping Tools software (Wessel & Smith 1991).

REFERENCES

Altamimi, Z., Collilieux, X. & Métivier, L., 2011. ITRF2008: an improved solution of the International Terrestrial Reference Frame, *J. Geodyn.,* **85,** 457–473, doi:10.1007/s00190-011-0444-49.

Argus, D.F., 2007. Defining the translational velocity of the reference frame of Earth, *Geophys. J. Int.,* **169,** 830–838, doi:10.1111j.1365-246X.2007.03344.x.

Benford, B. *et al.*, 2012. GPS estimates of microplate motions, northern Caribbean: evidence for a Hispaniola microplate and implications for earthquake hazard, *Geophys. J. Int.,* submitted.

Burke, K., Grippi, J. & Sengor, A.M.C., 1980. Neogene structures in Jamaica and the tectonic style of the northern Caribbean Plate boundary zone, *J. Geol.,* **88,** 375–386.

Calais, E. *et al*., 2010. Transpressional rupture of an unmapped fault during the 2010 Haiti earthquake, *Nature Geosci.,* **3,** doi:10.1038/NGEO992.

Clark, G.R., II, 1995. Swallowed up, *Earth,* **4,** 34–41.

DeMets, C. & Wiggins-Grandison, M., 2007. Deformation of Jamaica and motion of the Gônave microplate from GPS and seismic data, *Geophys. J. Int.,* **168,** 362–378, doi:10.1111/j.1365-246X.2006.03236.x.

DeMets, C., Mattioli, G., Jansma, P., Rogers, R.D., Tenorio, C. & Turner, H.L., 2007. Present motion and deformation of the Caribbean plate: constraints from new GPS geodetic measurements from Honduras and Nicaragua, in *Geologic and Tectonic Development of the Caribbean Plate in Northern-Central America,* Geol. Soc. Am. Spec. Paper, Vol. 428, pp. 21–36, doi:10.1130/2007.2428(02), ed. Mann, P., The Geological Society of America, Boulder, CO.

DeMets, C., Gordon, R.G. & Argus, D.F., 2010. Geologically current plate motions, *Geophys. J. Int.,* **181,** 1–80, doi:10.1111/j.1365256X .2009.04491.x.

Draper, G., 2008. Some speculations on the Paleogene and Neogene tectonics of Jamaica, *Geol. J.,* **43,** 563–572.

Genrich, J.F., Bock, Y., McCaffrey, R., Prawirodirdjo, L., Stevens, C.W., Puntodewo, S.S.O., Subarya, C. & Wdowinski, S., 2000. Distribution of slip at the northern Sumatran fault system, *Geophys. Res. Lett.,* **105,** 28 327–28 341, doi:10.1029/2000JB900158.

Grippi, J., 1978. Geology of the Lucea Inlier, western Jamaica, *M.S. thesis*. State University of New York at Albany, Albany, NY.

Hayes, G.P. *et al*., 2010. Complex rupture during the 12 January 2010 Haiti earthquake, *Nature Geosci.,* **3,** doi:10.1038/NGEO977.

Horsfield, W.T., 1974. Major faults in Jamaica, *J. Geol. Soc. Jamaica,* **14,** 1–15.

Jansma, P.E. & Mattioli, G.S., 2005. GPS results from Puerto Rico and the Virgin Islands: constraints on tectonic setting and rates of active faulting, in *Active Tectonics and Seismic Hazards of Puerto Rico, the Virgin Islands, and Offshore Areas,* Geol. Soc. Am. Spec. Paper, Vol. 385, pp. 13–30, doi:10.1130/2007.2428(02), ed. Mann, P., The Geological Society of America, Boulder, CO.

Leroy, S., Mercier de Lepinay, B., Mauffret, A. & Pubellier, M., 1996. Structural and tectonic evolution of the eastern Cayman Trough (Caribbean Sea) from seismic reflection data, *AAPG Bull.,* **80,** 222–247.

Manaker, D.M. *et al*., 2008. Interseismic plate coupling and strain partitioning in the northeastern Caribbean, *Geophys. J. Int.,* **174,** 889–903, doi:10.1111/j.1365-246X.2008.03819.x.

Mann, P. & Burke, K., 1990. Transverse intra-arc rifting: Palaeogene Wagwater Belt, Jamaica, *Mar. Pet. Geol.,* **7,** 410–427.

Mann, P., Draper, G. & Burke, K., 1985. Neotectonics of a strike-slip restraining bend system, Jamaica, in *Strike-Slip Deformation and Sedimentation, Special Publication, SEPM 37,* pp. 211–226, eds Biddle, K. & Christie-Blick, N., SEPM, Tulsa.

Mann, P., Schubert, C. & Burke, K., 1990. Review of Caribbean neotectonics, in *The Geology of North America, The Caribbean region,* pp. 307–338, eds Dengo, G. & Case, J.E.H., Geological Society of America, Boulder, CO.

Mann, P., Taylor, F.W., Edwards, R.L. & Ku, T.-L., 1995. Actively evolving microplate formation by oblique collision and sideways motion along strike-slip faults; an example from the northeastern Caribbean plate margin, *Tectonophysics,* **246,** 1–69.

Mann, P., Calais, E., Ruegg, J.-C., DeMets, C., Jansma, P. & Mattioli, G.S., 2002. Oblique collision in the northeastern Caribbean from GPS measurements and geological observations, *Tectonics,* **37,** doi:0.1029/2001TC001304.

Mann, P., DeMets, C. & Wiggins-Grandison, M., 2007. Toward a better understanding of the Late Neogene strike-slip restraining bend in Jamaica: geodetic, geological, and seismic constraints, in *Tectonics of Strike-Slip Restraining and Releasing Bends,* Geol. Soc. London Spec. Pub., Vol. 290, pp. 239–253, eds Cunningham, W.D. & Mann, P., Geological Society, London.

Marquez-Azua, B. & DeMets, C., 2003. Crustal velocity field of Mexico from continuous GPS measurements, 1993 to June 2001: implications for the neotectonics of Mexico, *J. geophys. Res.,* **108,** 2450, doi:10.1029/2002JB002241.

Meade, B.J. & Loveless, J.P., 2009. Block modeling with connected fault-network geometries and a linear elastic coupling estimator in spherical coordinates, *Bull. seism. Soc. Am.,* **99,** 3124–3139, doi:10.17850120090088.

Mitchell, S.F., 2003. Sedimentology and tectonic evolution of the Cretaceous rocks of central Jamaica: relationships to the plate tectonic evolution of the Caribbean, in *The Circum-Gulf of Mexico and the Caribbean: Hydrocarbon Habitats, Basin Formation, and Plate Tectonics,* AAPG Mem., Vol. 79, pp. 605–623, eds Bartolini, C., Buffler, R.T. & Blickwede, J., American Association of Petroleum Geologists, Tulsa, OK.

Natural Disaster Research, Inc., Earthquake Unit, Mines & Geology Division, 1999. Kingston Metropolitan Area Seismic Hazard Assessment Final Report, Caribbean Disaster Mitigation Project, Organization of American States. Available at: www.oas.org/cdmp/document/kma/seismic/kma1.htm, pp. 82 (last accessed 2007 September).

Pearson, C., Denys, P. & Hodgkinson, K., 2000. Geodetic constraints on the kinematics of the Alpine Fault in the southern South Island of New Zealand, using results from Hawea-Haast GPS transect, *Geophys. Res. Lett.,* **27,** 1319–1322, doi:10.1029/1999GL008412.

Pereira, J., 1977. An engineering seismology study of Jamaica, *MSc thesis,* Imperial College, London, 147pp.

Prentice, C.S., Mann, P., Crone, A.J., Gold, R.D., Hudnut, K.W., Briggs, R.W., Koehler, R.D. & Jean, P., 2010. Seismic hazard of the Enriquillo-Plantain Garden fault in Haiti inferred from palaeoseismology, *Nature Geosci.,* **3,** doi:10.1038/NGEO991.

Rosencrantz, E. & Mann, P., 1991. SeaMARC II mapping of transform faults in the Cayman Trough, Caribbean Sea, *Geology,* **19,** 690–693.

Sandwell, D.T. & Smith, W.H.F., 1997. Marine gravity anomaly from Geosat and ERS 1 altimetry, *J. geophys. Res.,* **102,** 10 039–10 054.

Spinler, J.C., Bennett, R.A., Anderson, M.L., McGill, S.F., Hreinsdottir, S. & McCallister, A., 2010. Present-day strain accumulation and slip rates associated with southern San Andreas and eastern California shear zone faults, *J. geophys. Res.,* **115,** B11407, doi:10.1029/2010JB007424.

Stein, S. & Gordon, R.G., 1984. Statistical tests of additional plate boundaries from plate motion inversions, *Earth planet. Sci. Lett.,* **69,** 401–412.

Taber, S., 1920. Jamaica earthquakes and the Bartlett Trough, *Bull. Seism. Soc. Am.,* **10,** 55–86.

Tomblin, J.M. & Robson, G.R., 1977. A catalogue of felt earthquakes for Jamaica, with references to other islands in the Greater Antilles, 1564–1971, Ministry of Mining and Natural Resources (Jamaica), Mines & Geology Division Special Publication No. 2, Kingston, Jamaica, 243pp.

Tyburski, S.A., 1992. Deformational mechanisms along active strike-slip faults: SeaMARC II and seismic data from the North America-Caribbean plate boundary, *MSc thesis,* University of Texas, Austin, TX, 194pp.

Van Dusen, S.R. & Doser, D.I., 2000. Faulting processes of historic (1917–1962) M $\geq$ 6.0 earthquakes along the north-central Caribbean margin, *Pure appl. Geophys.,* **157,** 719–736.

Versey, H.R., Williams, J.B. & Robinson, E., 1958. The earthquake of March 1, 1957, *Geonotes; Q Newsl. Jamaica Group Geologists Assoc.,* **1,** 54–65.

Wadge, G. & Dixon, T.H., 1984. A geological interpretation of SEASAT-SAR imagery of Jamaica, *J. Geol.,* **92,** 561–581.

Wessel, P. & Smith, W.H.F., 1991. Free software helps map and display data, *EOS, Trans. Am. geophys. Un.,* **72,** 441–446.

Wiggins-Grandison, M.D., 1996. Seismology of the January 1993 earthquake, *J. Geol. Soc. Jamaica,* **30,** 1–14.

Wiggins-Grandison, M.D., 2001. Preliminary results from the new Jamaica seismograph network, *Seism. Res. Lett.,* **72,** 525–537.

Wiggins-Grandison, M.D., 2004. Simultaneous inversion for local earthquake hypocenters, station corrections, and 1-D velocity model of the Jamaican crust, *Earth planet. Sci. Lett.,* **224,** 229–240.

Wiggins-Grandison, M.D. & Atakan, K., 2005. Seismotectonics of Jamaica, *Geophys. J. Int.,* **160,** 573–580, doi:10.1111/j.1365-246X.2004.02471.x.

Wright, R.M., 1975. Aspects of the geology of Tertiary limestones in west-central Jamaica, *PhD thesis,* Stanford University, Stanford, CA, 320pp.

Zumberge, J.F., Heflin, M.B., Jefferson, D.C., Watkins, M.M. & Webb, F.H., 1997. Precise point positioning for the efficient and robust analysis of GPS data from large networks, *J. geophys. Res.,* **102,** 5005–5017.